

# DESIGN OF THE SHIP-BORNE MULTI-WAVELENGTH POLARIZATION OCEAN LIDAR SYSTEM AND MEASUREMENT OF SEAWATER OPTICAL PROPERTIES

Qi Liu<sup>1</sup>, Bingyi Liu<sup>1,2</sup>, Songhua Wu<sup>1,2\*</sup>, Jintao Liu<sup>1</sup>, Kailin Zhang<sup>1</sup>, Xiaoquan Song<sup>1,2</sup>,  
Xiangcheng Chen<sup>1</sup>, Peizhi Zhu<sup>1</sup>

<sup>1</sup> Ocean Remote Sensing Institute, College of Information Science and Engineering, Ocean University of China, Qingdao 266100, China

<sup>2</sup> Laboratory for Regional Oceanography and Numerical Modeling, Pilot National Laboratory for Marine Science and Technology (Qingdao), Qingdao 266237, China

\*Email: wush@ouc.edu.cn

## ABSTRACT

A ship-borne multi-wavelength polarization ocean lidar system LOOP (Lidar for Ocean Optics Profiler) is introduced in detail, aiming to obtain high-precision vertical profiles of seawater optical characteristics. Based on Monte-Carlo simulation, the receiving telescope is designed with a variable field of view, producing system attenuation coefficient ( $K_{\text{lidar}}$ ) approximating the optical parameters of seawater under a different field of view and water body conditions. At first, a sea trial was conducted in Jiaozhou Bay, and the measured diffuse attenuation coefficient ( $K_d$ ) of seawater was  $0.3\text{m}^{-1}$ , being in good agreement compared with the results measured by field instrument TriOS. Then a field campaign was organized in the South China Sea. The measurement of the seawater diffuse attenuation ( $K_d$ ) was  $0.035\text{m}^{-1}$ . These results support the prospects that lidar, as an effective tool supplement to traditional passive ocean color remote sensing, can provide the vertical distributions of optical properties in the upper ocean.

## 1. INTRODUCTION

Ocean Color Sciences is an important part of Earth observation. The results of measurement and analysis have revolutionized the field of biological oceanography and have made important contributions to biogeochemistry, physical oceanography, ocean systems models, marine fisheries and coastal zone management [1][2]. The optical properties of solutes and particles in seawater vary with the type and concentration, which decides the optical properties of seawater showing great spatial and temporal changes. The optical properties of seawater have a strong

relationship with biological, chemical, geographic and physical environments, which determine that the Ocean optics is the basis and key role of the Ocean Color Sciences and the Remote Sensing [3]. At present, the measurement of the inherent optical properties of seawater mainly uses the in-situ optical cage and passive ocean color satellite [4]. The in-situ optical cage can only measure several profiles per day, which is difficult to perform large-scale measurements in a short period of time and cannot fully characterize the temporal and spatial variation of ocean optical properties. Passive ocean color satellites can only observe during the daytime, and the observed results are affected by atmospheric correction, having large errors. Besides, the inversion algorithm is based on the assumption that the seawater is vertically uniform, and the vertical profile information of the ocean optical properties cannot be given [5].

Lidar using the blue-green band laser can easily penetrate the water body, which can directly and accurately obtain the high-precision vertical profile of seawater optical properties [6], thus making up for the limitations of in-situ optical cages and passive ocean color satellites, achieving breakthrough from 2D plane to 3D stereoscopic observation.

For the anticipation, this paper describes in detail of the self-developed ship-borne multi-wavelength polarized lidar system, LOOP (Lidar for Ocean Optics Profiler), in Sect.2. The results in Jiaozhou Bay and the South China Sea and case studies are provided in Sect. 3.

## 2. METHODOLOGY

### 2.1 The lidar system

Utilizing three-wavelength Nd:YAG narrow pulse laser with high energy, the LOOP system has five regular channels including 355 nm parallel-cross polarization, 532 nm parallel-cross polarization and 1064nm. The wavelength of 355nm is used for fluorescence. The backscattered light at the wavelength of 532nm is used for ocean optical properties. Both wavelengths of 532nm and 355nm with parallel-cross polarization are used for particle recognition obtained by the depolarization ratio. The water surface distance is measured at the 1064-nm wavelength. The LOOP system specifications are shown in Table 1.

Laser	wavelength(nm)	355&532&1064
	Pulse energy (mj)	1064nm@400
		532nm@200
		355nm@120
	Repetition rate(Hz)	20
	Pulse duration (ns)	≤5
Divergence(mrad)	≤0.5	
Receiver	Aperture(mm)	60
	Field(mrad)	5~100
	Filter_FWHM(nm)	2
	Sampling frequency	AD@250MHz
		PC@1GHz

Table 1. LOOP system hardware configuration.

Based on the Monte Carlo simulation, the lidar system attenuation coefficient  $K_{lidar}$ , is close to different ocean water optical properties in the different fields of view [7]. As shown in Fig.1, the telescope is designed with a set of lens and a variable stop located behind the aspherical lens is used to control the system's field of view from 5mrad to 100mrad. The return signal travels to the five regular channels through beam splitters and narrow-band interference filters positioned at the front of photomultiplier tubes (PMT). Besides, the 420nm-700nm spectrum channel is reserved for the future detection of hyper fluorescence signals in seawater.

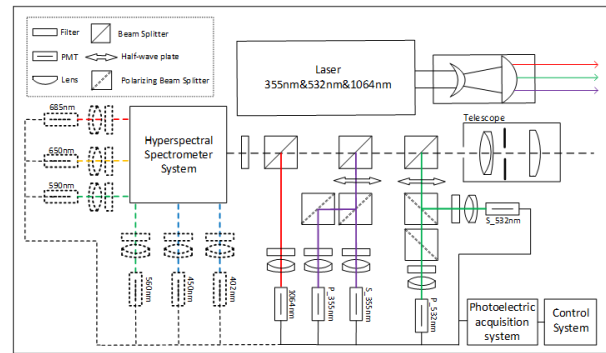


Fig 1. The LOOP system.

Notice that at front of the polarizing beam splitters (PBS) of 355nm and 532nm, a half-wave plate was used for the method called “ $\Delta 45^\circ$ -calibration” to calibrate the volume linear depolarization ratio [8]. And at the cross polarization channels of 355nm and 532nm, the PBS equipped to ensure  $T_p/T_s$  extinction ratio cube reaches  $10^6:1$ . Finally, the return signals were recorded by independent research and development of digitizer at a sampling rate of 1 GHz for photon counting (PC) and 250MHz for analog with 14-bit digitally resolution.

## 2.2 Method

The LOOP was initially field tested aboard a boat in Jiaozhou Bay on July 30, 2018. A field instrument TriOS measured the seawater diffuse attenuation ( $K_d$ ) simultaneously. Then the system was deployed aboard the No.9 Marine Geology research ship in the South China Sea for four days trial (March 7 to 10, 2019, Fig.2).



Fig 2. LOOP field experiment. The left is in Jiaozhou Bay and the right is in the South China Sea.

For the ship-borne ocean lidar, the return signal can be expressed as [9]:

$$P(z) = \frac{A\beta(z)}{n(nH+z)^2} \exp \left[ -2 \int_0^z K_{lidar}(y) dy \right] \quad (1)$$

Where  $z$  is depth,  $A$  is a calibration factor including geometric losses, incidence of the sea surface and two-way transmission through sea surface,  $n$  is the refractive index of sea water,  $H$  is the distance from the lidar to the surface,  $z$  is the path length in water,  $\beta$  is the volume scattering coefficient at a scattering angle of  $\pi$  radians and  $K_{\text{lidar}}$  is the lidar attenuation coefficient.

The system attenuation coefficient ( $K_{\text{lidar}}$ ) was calculated using the slope method [10]. This method derives both  $\beta$  and  $K_{\text{lidar}}$  from the signal. But considering the ocean optical conditions, there is an approximation algorithm. If the water column is well mixed in the upper ocean [11], both  $K_{\text{lidar}}$  and  $\beta$  will be constant over the profile. In this case,  $K_{\text{lidar}}$  can be derived from the slope of the logarithm of the signal.

### 3. RESULTS

#### 3.1 Jiaozhou Bay (near-shore water)

The prototype of the LOOP system was first compared with the field instrument TriOS (field instrument) to obtain the optical properties profile of the coastal water column on July 30, 2018.

Due to the turbidity of the coastal water column and large dynamic range of the return signal, it is difficult to improve laser effective penetration depth. As the system was deployed above water on the boat, when the laser emitted with high energy, the specular return off the sea surface cause digitizer saturation that cannot obtain the signal of the water column even to 20m below the surface. Otherwise, the laser energy rapidly with depth, making the effective penetration only 5m. Finally, the lidar measurement of  $K_{\text{lidar}}$  in the range from 3.6m to 7.8m was selected for comparison with the TriOS measurement of  $K_d$  in the range from 0.8m to 5.8m.

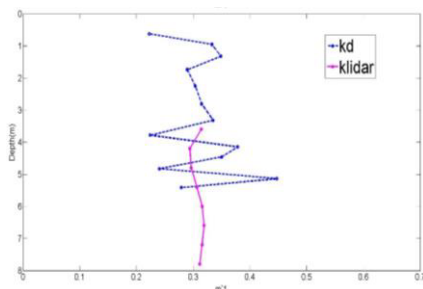


Fig 3.  $K_{\text{lidar}}$  compared with  $K_d$  measured by field instrument TriOS

#### 3.2 The South China Sea (off-shore water)

A field campaign was organized on March 10, 2019, in the South China Sea. Fig 4. shows the lidar attenuated backscatter for two different fields of view. A strong saturation from the water surface to 18m underwater was found when the field of view is 100mrad. It can easily be observed that the signal decayed more rapidly in the narrow field of view than in wide one.

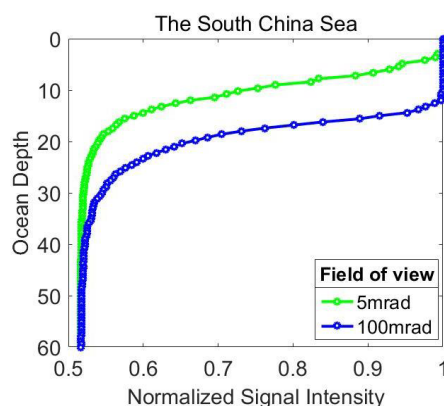


Fig 4. Lidar attenuated backscatter in the narrow field of view (5mrad) and wide field of view (100mrad).

Fig 5. Shows the  $K_{\text{lidar}}$  derived from above lidar attenuated backscattering. In the narrow field of view,  $K_{\text{lidar}}$  has a large value initially then decayed to the same value as the wide field of view. It is considered that  $K_{\text{lidar}}$  in both fields of view tends to be diffuse attenuation coefficient  $K_d$  around  $0.035 \text{ m}^{-1}$  below 40m depth of water column. The perturbation which did not do any smoothing may be caused by strong winds and ocean waves on the day. And the backscatter response is expressed as the combination of convolution in terms of the water column and strong reflection of the sea surface, which caused  $K_{\text{lidar}}$  a large error above the water depth of 18m.

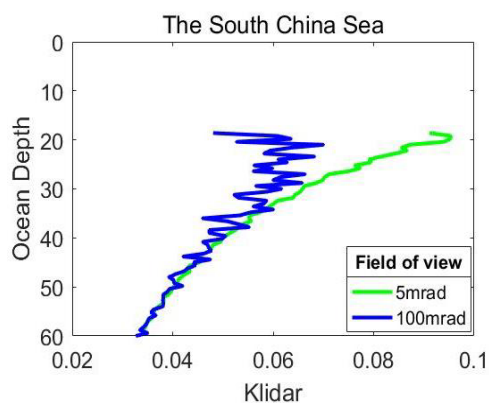


Fig 5. Measurement of  $K_{\text{lidar}}$  in the different field of view.

#### 4. Discussion

These results support the proposition that the ship-borne ocean lidar can provide an effective way to obtain the vertical distributions of optical properties and geochemical constituents for remotely measuring in the upper ocean. However, in order to improve the detection capability of ocean lidar, there are many challenges. Most important, for example, the up to  $10^{10}$  dynamic range of the lidar signal transmission to 70m needs a high-speed digitizer with sufficient dynamic range. Even though there are several approaches to maximizing dynamic range, all of them have advantages or disadvantages. In addition, the Gaussian laser beam transmits in the water column with a larger divergence, limiting the laser penetration depth of the seawater column. A new approach such as the Bessel beam may be an ideal way to solve this problem. Furthermore, the Optical Parametric Oscillator (OPO) laser which can emit tunable laser wavelength with higher energy and repetition rate should develop because of different types of water columns having a different optimal optical penetration window. Farther into the longer term with the development of lidar, global ocean coverage from a satellite oceanographic lidar is likely. The measurement of the absorption coefficient  $a$ , backscatter coefficient  $b$ , plankton layers and particulates discrimination related to depolarization will be investigated in the future.

#### ACKNOWLEDGEMENTS

This research was funded by National Key Research and Development Program of China, grant number 2016YFC1400904, supported by Pilot National Laboratory for Marine Science and Technology (Qingdao).

#### REFERENCES

- [1] Behrenfeld M J, et al., *Nature Climate Change*, 2016, 6(3): 323-330.
- [2] Dutkiewicz S, et al., *Nature Communications*, 2019, 10(1).
- [3] McClain C R, et al., *Experimental Methods in the Physical Sciences*, 2014, 47:73-119.
- [4] Lee Z, et al., *Applied Optics*, 57, 3463-3473 (2018).
- [5] Lu X, et al., *Journal of Geophysical Research: Oceans*, 2014, 119(7): 4305-4317.
- [6] Churnside J H, et al., *Applied Optics*, 1998, 37(15): 3105-3112.
- [7] Gordon H R, *Applied Optics*, 1982, 21(16): 2996-3001.
- [8] Dai G, et al., *Remote Sensing*, 2018;10(3).
- [9] Churnside J H, *Optical Engineering*, 2013, 53(5):051405.
- [10] Churnside J H, et al., *Applied Optics*, 2017;56 (18):5228-33.
- [11] C de Boyer, et al., *Journal of Geophysical Research*, 2004, 109(C12).